INTERNATIONAL JOURNAL FOR NUMERICAL METHODS IN FLUIDS
Int. J. Numer. Meth. Fluids 2009; **60**:391–408
Published online 13 August 2008 in Wiley InterScience (www.interscience.wiley.com). DOI: 10.1002/fld.1896

A high-resolution wetting and drying algorithm for free-surface hydrodynamics

Vincenzo Casulli*, †

Laboratory of Applied Mathematics, Department of Civil and Environmental Engineering, University of Trento, 38050 Mesiano, Trento, Italy

SUMMARY

A new wetting and drying algorithm for numerical modeling free-surface flows is proposed and analyzed. A well structured, mildly nonlinear system for the discrete water surface elevation is derived from the governing differential equations by requiring a correct mass balance in wet areas as well as in the region of transition from wet to dry and from dry to wet. Existence and uniqueness of the numerical solution, along with a convergence analysis of an iterative scheme for the mildly nonlinear system, is provided. The present algorithm is devised to use high-resolution bathymetric data at subgrid level. The resulting model is quite efficient, does not require a threshold value for minimal water depth, does not produce un-physical negative water depths and generates accurate results with relatively coarse mesh and large time step size. These features are illustrated on a severe test-case with known analytical solution. Copyright © 2008 John Wiley & Sons, Ltd.

Received 4 December 2007; Revised 27 May 2008; Accepted 13 July 2008

KEY WORDS: wetting and drying; shallow water equations; finite volume; subgrid resolution; semi-implicit; free-surface

1. INTRODUCTION

In most numerical models for free-surface flows, which are based on fixed grids, wetting and drying is usually controlled by artificially placing 'screens' in velocity points of the grid when the water depth drops below a certain *drying threshold*, and removing the screens when the water depth rises above a *flooding threshold*. When a screen is placed, the flow velocity is set to zero and the point is taken out of the computation. Once a numerical method for the governing differential equations has been chosen, the different wetting and drying algorithms mainly differ in the criterions used for determining when a grid point becomes dry or is wetted again.

*Correspondence to: Vincenzo Casulli, Laboratory of Applied Mathematics, Department of Civil and Environmental Engineering, University of Trento, 38050 Mesiano, Trento, Italy.
†E-mail: vincenzo.casulli@unitn.it

Screen and threshold approaches are often derived from professional experience and are not always supported by a rigorous mathematical derivation. Consequently, the accuracy of the numerical results is sometimes questionable and has to rely on problem-dependent threshold parameters to be tuned. Use of a drying threshold, for example, implies that a substantial water volume may remain trapped in the dry region of the simulation domain. In addition, inaccurate wave reflection from the approximated shoreline unavoidably propagates to deeper water.

A vast literature dealing with the numerical treatment of wetting and drying is available (see, e.g. [1, 2] and the numerous references contained therein). A pioneer numerical model based on the two-dimensional shallow water equations that was devised to simulate wetting and drying was proposed by Leendertse in 1970 [3]. This model uses an alternating direction implicit method to discretize the governing differential equations and has been extensively studied by several authors (see, e.g. [4–6]).

Some semi-implicit methods for the two- and three-dimensional shallow water equations do not use a drying threshold [7–9]. Consequently, no water gets trapped in the dry region but the resulting water depths in the drying process may become negative. This problem has been recently investigated in [10] where a sufficient condition for a semi-implicit method to produce nonnegative water depths was derived. This condition essentially requires that the velocity Courant number in the drying area is restricted to be smaller than 1.

The time step size plays an important role also in wetting dry surfaces because when a relatively large time step is used, artificial bores that travel at a limited speed of one cell per time step may be generated. Thus, again, the time step size needs to be limited by a maximum velocity Courant number of 1 so that the front cannot propagate faster than one cell per time step [11]. To overcome this limitation the concept of 'artificial porosity' has been proposed in [6]. Artificial porosity, however, introduces a number of side effects including an increase of the actual wave speed in the wetting and drying region where the water depth falls below a specified threshold.

A time step limitation imposing the velocity Courant number to be smaller than 1, together with the use of a refined mesh in the wetting and drying region, easily result in an excessive and unnecessary computational effort.

In the present study a new wetting and drying algorithm is directly derived from the governing differential equations and becomes a substantial part of the resulting numerical method. The discrete free-surface equation has been revised in order to correctly represent the precise mass balance in areas of transition from wet to dry or from dry to wet. The resulting system, rather than being linear, is *mildly nonlinear*, but rigorous mass conservation and nonnegative water depths are guaranteed everywhere and for any time step size. It will be shown that no additional cost is required by the present algorithm when the computational domain is everywhere wet. A few extra iterations are needed to solve the mildly nonlinear system when a wetting and drying dynamic is present.

Moreover, enhanced accuracy is obtained with the specification of bathymetric details at subgrid level, so that excessive and costly grid refinement can be avoided. Any computational cell is allowed to be wet, partially wet or dry. A dry point is recognized by having precisely zero water depth that is obtained without the use of a drying threshold. The wetting and drying process may involve several cells within the same time step.

For simplicity, the present derivation is based only on a two-dimensional, vertically averaged version of a previously formulated numerical model that uses a semi-implicit finite volume discretization of the three-dimensional shallow water equations [9]. The present algorithm naturally extends to three-dimensional hydrostatic models as well as to nonhydrostatic models (see,

DOI: 10.1002/fld

e.g. [12]). In this latter case the correct volume balance in areas of transition from wet to dry and from dry to wet is obtained by solving an additional mildly nonlinear system for the nonhydrostatic pressure component.

The remainder of this paper is organized as follows. In Section 2 the governing differential equations, the unstructured orthogonal grid and the mathematical specifications for an arbitrary subgrid resolution are given. A consistent finite volume discretization that leads to a mildly nonlinear system of equations for the water surface elevation is given in Section 3. Next, an efficient Newton-type algorithm for solving the mildly nonlinear system is presented and discussed in Section 4. Finally, a severe numerical test is given in Section 5 to emphasize the validity and the importance of the proposed algorithm.

2. MODEL FORMULATION FOR WETTING AND DRYING

2.1. Governing equations

The well known, vertically averaged shallow water equations express the physical principles of momentum and mass conservation. These equations can be written in the following form:

$$H(u_t+uu_x+vu_y-fv)=-gH\eta_x+[(\nu Hu_x)_x+(\nu Hu_y)_y]-\gamma u \tag{1}$$

$$H(v_t+uv_x+vv_y+fu)=-gH\eta_y+[(\nu Hv_x)_x+(\nu Hv_y)_y]-\gamma v \tag{2}$$

$$H_t+(Hu)_x+(Hv)_y=0 \tag{3}$$

where $H(x,y,t)=h(x,y)+\eta(x,y,t)$ is the total water depth, $\eta(x,y,t)$ is the water surface elevation measured from the undisturbed water surface and $h(x,y)$ is a bounded function representing the prescribed bathymetry; $u(x,y,t)$ and $v(x,y,t)$ are the vertically averaged velocity components in the horizontal x- and y-directions, respectively; t is the time; f is the Coriolis parameter; g is the gravitational acceleration; ν is a nonnegative coefficient of eddy viscosity; and γ is a nonnegative bottom friction coefficient, which can be given by the Manning–Chezy formula.

When wetting and drying is expected, the differential equations (1)–(3) are defined on a time-dependent domain $\Omega(t)$ defined as $\Omega(t)=\{(x,y):H(x,y,t)>0\}$. Thus, $\Omega(t)$ is itself one of the unknowns to be determined numerically.

At the initial time $t=0$ the field variables $u(x,y,0)$, $v(x,y,0)$ and $\eta(x,y,0)$ are assumed to be known everywhere in $\Omega(0)$ as initial conditions.

2.2. Unstructured orthogonal grid

To solve Equations (1)–(3) numerically, a fixed domain Ω is chosen in such a fashion that $\Omega(t)\subseteq\Omega$ for all $t\geqslant 0$. Ω is then covered by an *unstructured orthogonal grid* [9] consisting of N_p nonoverlapping convex polygons $\Omega_i, i=1,2,\ldots,N_p$. Each side of a polygon is either a boundary line or a side of an adjacent polygon. Within each polygon a *center* must be identified in such a way that the segment joining the centers of two adjacent polygons and the side shared by the two polygons, have a nonempty intersection and are *orthogonal* to each other (see Figure 1).

Once Ω has been covered with an unstructured orthogonal grid, each polygon Ω_i may have an arbitrary number of sides $S_i\geqslant 3$. Let N_s be the total number of sides in the grid, and let λ_j, $j=1,2,\ldots,N_s$ be the length of each side. The sides of the ith polygon are identified by an index

DOI: 10.1002/fld

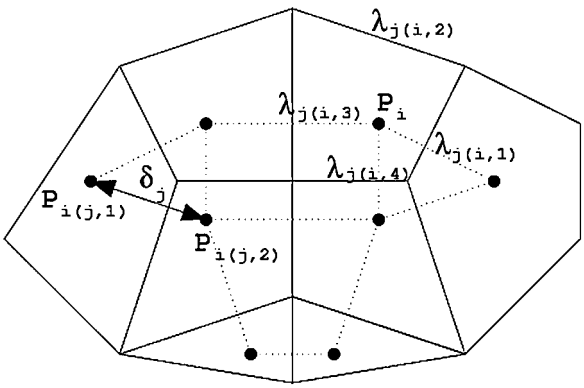

Figure 1. Unstructured orthogonal grid.

$j(i,\ell)$ so that $1\leqslant j(i,\ell)\leqslant N_s, \ell=1,2,\ldots,S_i$. Similarly, the two polygons that share the jth side of the grid are identified by the indices $i(j,1)$ and $i(j,2)$ so that $1\leqslant i(j,1)\leqslant N_p$ and $1\leqslant i(j,2)\leqslant N_p$. Let P_i be the area of the ith polygon. Moreover, $n(i,\ell)$ denotes the neighbor of polygon i that shares the side $j(i,\ell)$ with the ith polygon, hence $1\leqslant n(i,\ell)\leqslant N_p, \ell=1,2,\ldots,S_i$. The nonzero distance between the centers of two adjacent polygons which share the jth side is denoted with δ_j.

The discrete velocities and water surface elevation are defined at staggered locations as follows. The water surface elevation η_i^n, assumed to be constant within each polygon, is located at the center of the ith polygon; the velocity component u_j^n normal to the jth edge, assumed to be constant over the edge, is defined at the intersection between the edge and the segment joining the centers of the two polygons which share the edge.

2.3. Subgrid resolution

In presence of wetting and drying, use of a fixed unstructured grid alone is insufficient for fitting boundaries because the boundary is itself moving and unknown *a priori*. To overcome this difficulty, and for any specified bathymetry $h(x,y)$, a precise description of the flow domain that allows for arbitrary subgrid resolution will be expressed in terms of the auxiliary *porosity* function $p(x,y,z)$ defined by

$$p(x,y,z)=\begin{cases}1 & \text{if } h(x,y)+z>0,\\ 0 & \text{otherwise}\end{cases}\qquad (x,y)\in\Omega,\ \ -\infty<z<\infty \tag{4}$$

whose horizontal integral evaluated at $z=\eta_i^n$ within each polygon is given by

$$p_i(\eta_i^n)=\int_{\Omega_i} p(x,y,\eta_i^n)\,\mathrm{d}x\,\mathrm{d}y \tag{5}$$

and represents the free-surface area. Equation (4) implies that $p_i(\eta_i^n)$ is nonnegative, nondecreasing and bounded. Specifically, $0\leqslant p_i(\eta_i^n)\leqslant P_i$. Clearly, when $p_i(\eta_i^n)=0$ the ith polygon is dry; when $p_i(\eta_i^n)=P_i$ it is wet; and when $0<p_i(\eta_i^n)<P_i$ the ith polygon is *partially* wet.

DOI: 10.1002/fld

At each point within the ith polygon the total water depth is given by

$$H(x, y, \eta_i^n) = \int_{-\infty}^{\eta_i^n} p(x, y, z)\, \mathrm{d}z = \max[0, h(x, y) + \eta_i^n] \tag{6}$$

so that, $H(x, y, \eta_i^n) \geqslant 0$, and strict inequality identifies a wet point. Thus, the wet region within the ith polygon is given by

$$\Omega_i^n = \{(x, y) \in \Omega_i : H(x, y, \eta_i^n) > 0\} \tag{7}$$

The water volume within the ith polygon can be expressed either as an horizontal integral of the total water depth, or as a vertical integral of the surface area, and is given by

$$V_i(\eta_i^n) = \int_{-\infty}^{\eta_i^n} p_i(z)\, \mathrm{d}z = \int_{\Omega_i} H(x, y, \eta_i^n)\, \mathrm{d}x\, \mathrm{d}y \tag{8}$$

Thus, because $p_i(z)$ is nonnegative and nondecreasing, one has $V_i(\eta_i^n) \geqslant 0$ and strict inequality necessarily implies $p_i(\eta_i^n) > 0$. Moreover, the nonnegative cell-averaged water depth can be defined as $H_i^n = V_i(\eta_i^n)/P_i$.

Finally, by denoting with $x(s)$ and $y(s)$ the parametric coordinates of a point on the jth edge connecting the two vertices identified by the parameters $s = s_j^1$ and $s = s_j^2$, for a specified constant water level η_j^n along the jth edge, the corresponding wet cross-section area is given by

$$A_j(\eta_j^n) = \int_{s_j^1}^{s_j^2} H(x(s), y(s), \eta_j^n)\, \mathrm{d}s \tag{9}$$

so that the nonnegative edge-averaged water depth can be defined as $H_j^n = A_j(\eta_j^n)/\lambda_j$.

3. A SEMI-IMPLICIT FINITE VOLUME DISCRETIZATION

3.1. Horizontal momentum

An efficient semi-implicit scheme whose stability is independent from the free-surface wave speed, vertical viscosity and bottom friction was derived in [9] for the three-dimensional shallow water equations. This method also solves the two-dimensional shallow water equations in the particular case that only one vertical layer is specified. In this scheme, the water surface elevation in the momentum equations (1)–(2), and the velocity in the vertically integrated continuity equation (3), are discretized by the θ-method. Additionally, the bottom friction terms are discretized implicitly for stability purpose.

Following the guidelines given in [9], since Equations (1)–(2) are invariant under solid rotation of the x- and y-axis on the horizontal plane, a consistent semi-implicit finite difference discretization for the velocity component normal to each edge can be written as

$$H_j^n u_j^{n+1} = H_j^n G_j^n - \theta g H_j^n \frac{\Delta t}{\delta_j} [\eta_{i(j,2)}^{n+1} - \eta_{i(j,1)}^{n+1}] - \Delta t \gamma_j^n u_j^{n+1} \tag{10}$$

where the positive direction for u_j^n has been chosen to be from $i(j, 1)$ to $i(j, 2)$; G_j^n is an explicit finite difference operator that accounts for the explicit contributions from the discretization of the

DOI: 10.1002/fld

Coriolis, advection, viscosity and hydrostatic pressure. A particular form for G_j^n can be given in several ways, such as by using an Eulerian–Lagrangian approach (see, e.g. [8, 9]). In this case G_j^n can be defined as follows:

$$G_j^n = \frac{[1-\theta(1-\theta)f^2\Delta t^2]u_j^* + f\Delta t v_j^*}{1+\theta^2 f^2 \Delta t^2} + (1-\theta)g\frac{\Delta t}{\delta_j}[\eta_{i(j,2)}^n - \eta_{i(j,1)}^n] + \Delta t \Delta_h u_j^*$$

where u_j^* denotes the velocity component normal to the jth side of the grid and v_j^* is the tangential velocity component in a right-hand coordinate system. Both components are interpolated at time t_n at the end of the Lagrangian trajectory based on the values at adjacent grid points. The Lagrangian trajectory is calculated by integrating the velocity backwards in time from node j at t^{n+1} to its location at time t^n. Δ_h is the Laplacian discretization. Finally, θ is an implicitness factor to be taken in the range $\frac{1}{2} \leqslant \theta \leqslant 1$ (see [13]); and γ_j^n is the edge-averaged bottom friction coefficient.

Of course, Equation (10) is defined only at wet edges, i.e. where $H_j^n > 0$. On dry edges one has $H_j^n = 0$ and, accordingly, $u_j^{n+1} = 0$ is assumed. On wet edges, Equation (10) is a linear equation that involves the unknowns u_j^{n+1}, $\eta_{i(j,1)}^{n+1}$ and $\eta_{i(j,2)}^{n+1}$. Hence the new free-surface elevation needs to be computed in order to determine the new velocity field.

3.2. Mass conservation

Having assumed a constant free-surface elevation on each water column, upon integration of the free-surface Equation (3) over Ω_i, a semi-implicit *finite volume* discretization within each polygon is given by

$$V_i(\eta_i^{n+1}) = V_i(\eta_i^n) - \Delta t \sum_{\ell=1}^{S_i} s_{i,\ell} A_{j(i,\ell)}^n [\theta u_{j(i,\ell)}^{n+1} + (1-\theta) u_{j(i,\ell)}^n] \tag{11}$$

where $V_i(\eta_i^n)$ is the water volume in the ith water column delimited by the surface elevation η_i^n, $A_j^n = A_j(\eta_j^n)$, and $s_{i,\ell}$ is a sign function associated with the orientation of the normal velocity defined on the ℓth side of polygon i. Specifically, $s_{i,\ell} = 1$ if a positive velocity on the ℓth side corresponds to outflow, $s_{i,\ell} = -1$ if a positive velocity on the ℓth side corresponds to inflow to the ith polygon. Thus, since either $i[j(i,\ell),1] = i$ or $i[j(i,\ell),2] = i$, $s_{i,\ell}$ can be written as

$$s_{i,\ell} = \frac{i[j(i,\ell),2] - 2i + i[j(i,\ell),1]}{i[j(i,\ell),2] - i[j(i,\ell),1]}$$

The new field variables u_j^{n+1} and η_i^{n+1} and the corresponding wet domain Ω^{n+1} are determined by solving together Equations (10) and (11) at each time step. To this purpose, formal substitution of the expressions for u_j^{n+1} from Equation (10) into (11) yields a nonlinear finite volume equation for η_i^{n+1} which is given by

$$\begin{aligned} &V_i(\eta_i^{n+1}) - g\Delta t^2 \theta^2 \sum_{\ell=1}^{S_i} \frac{\lambda_{j(i,\ell)}}{\delta_{j(i,\ell)}} \left(\frac{H^2}{H+\Delta t\gamma}\right)_{j(i,\ell)}^n (\eta_{n(i,\ell)}^{n+1} - \eta_i^{n+1}) \\ &= V_i(\eta_i^n) - \Delta t \sum_{\ell=1}^{S_i} s_{i,\ell} \lambda_{j(i,\ell)} H_{j(i,\ell)}^n \left[\theta \frac{HG}{H+\Delta t\gamma} + (1-\theta)u\right]_{j(i,\ell)}^n, \quad i = 1, 2, \ldots, N_p \end{aligned} \tag{12}$$

DOI: 10.1002/fld

It is to be noted that in those polygons i, where $H^n_{j(i,\ell)}=0$ for all $\ell=1,2,\ldots,S_i$, Equation (12) trivially implies $V_i(\eta_i^{n+1})=V_i(\eta_i^n)$, thus $\eta_i^{n+1}=\eta_i^n$ can be assumed. In this case, Equation (12) does not contribute to the system that is being formulated. The remaining set of Equations (12) (where at least one of $H^n_{j(i,\ell)}$ is nonzero) can be assembled into a *mildly nonlinear*, sparse system of N_η equations for η_i^{n+1}, with $N_\eta \leqslant N_p$. Details of a convergent iterative scheme to solve this system will be elaborated in the following section.

Once the new free-surface elevations η_i^{n+1} have been computed, the discrete velocities u_j^{n+1} are readily obtained from Equation (10) throughout the computational domain. Moreover, the new wet areas $p_i(\eta_i^{n+1})$, the water depths $H(x,y,\eta_i^{n+1})$, the wet regions Ω_i^{n+1} and the new water volumes $V_i(\eta_i^{n+1})$ are given by Equations (5)–(8) after replacing n with $n+1$. Clearly, for all $i=1,2,\ldots,N_p$ one has $0\leqslant p_i(\eta_i^{n+1})\leqslant P_i$, $H(x,y,\eta_i^{n+1})\geqslant 0$, $\Omega_i^{n+1}\subseteq\Omega_i$ and $V_i(\eta_i^{n+1})\geqslant 0$. Moreover, the overall wet region is given by

$$\Omega^{n+1}=\bigcup_{i=1}^{N_P}\Omega_i^{n+1} \tag{13}$$

Finally, in order to update the wet cross-section areas $A_j(\eta_j^{n+1})$ from Equation (9), the free-surface elevations η_j^{n+1} at polygon edges can be derived from the newly computed $\eta_{i(j,1)}^{n+1}$ and $\eta_{i(j,2)}^{n+1}$ by various criteria (mean, max, upwind). Then, the new edge-averaged water depth is given by $H_j^{n+1}=A_j(\eta_j^{n+1})/\lambda_j$.

4. SOLUTION ALGORITHM

4.1. A mildly nonlinear system for the free-surface

The newly proposed finite volume formulation (11) leads to the mildly nonlinear system of N_η Equation (12) for the discrete free-surface elevation η^{n+1}. The nonlinearity resides in the definition of the water volumes $V_i(\eta_i^{n+1})$ given by Equation (8). This large system needs to be solved at every time step with an efficient iterative scheme whose convergence can be guaranteed under physically compatible assumptions. With this objective existence and uniqueness of the solution, along with a converging Newton-type scheme, will be provided and analyzed in this section. To this purpose, system (12) is first written in a more compact vector notation as

$$\mathbf{V}(\zeta)+\mathbf{T}\zeta=\mathbf{b} \tag{14}$$

where

$$\zeta=\begin{bmatrix}\eta_1^{n+1}\\ \eta_2^{n+1}\\ \vdots\\ \eta_{N_\eta}^{n+1}\end{bmatrix},\quad \mathbf{V}(\zeta)=\begin{bmatrix}V_1(\zeta_1)\\ V_2(\zeta_2)\\ \vdots\\ V_{N_\eta}(\zeta_{N_\eta})\end{bmatrix}$$

DOI: 10.1002/fld

T is the sparse and symmetric $N_\eta \times N_\eta$ matrix that arises from the second term on the left-hand side of Equation (12) and **b** is a vector with N_η elements given by the right-hand sides of Equation (12). Without loss of generality, it will be assumed that $N_\eta = N_p$ and that matrix **T** is irreducible. This may not be the case when, at any time, two or more wet sub-domains of Ω^n are not connected. In such a circumstance the considerations that follow apply separately to each such sub-domain where the corresponding matrix **T** is irreducible. For the time being, it will also be assumed that Ω^n does not have open boundaries, so that at the boundary edges one has $A_j^n = H_j^n = 0$.

The ith main-diagonal element of matrix **T** is the coefficient of η_i^{n+1} in Equation (12) and is given by

$$t_{i,i} = g\Delta t^2\theta^2 \sum_{\ell=1}^{S_i} \frac{\lambda_{j(i,\ell)}}{\delta_{j(i,\ell)}} \left(\frac{H^2}{H+\Delta t\gamma}\right)^n_{j(i,\ell)}$$

The possibly nonzero off-diagonal elements in each row of matrix **T** are the coefficients of $\eta_{n(i,\ell)}^{n+1}$ in Equation (12), and are given by

$$t_{i,n(i,\ell)} = -g\Delta t^2\theta^2 \frac{\lambda_{j(i,\ell)}}{\delta_{j(i,\ell)}} \left(\frac{H^2}{H+\Delta t\gamma}\right)^n_{j(i,\ell)}, \quad \ell = 1, 2, \ldots, S_i$$

Since $H \geqslant 0$ and $\gamma \geqslant 0$, one has $t_{i,n(i,\ell)} \leqslant 0$ for all $\ell = 1, 2, \ldots, S_i$. Moreover, because **T** is irreducible, for each $i = 1, 2, \ldots, N_p$, at least one of $t_{i,n(i,\ell)}$ is nonzero. Consequently, $t_{i,i} > 0$.

From the above considerations it can be concluded that **T** is an irreducible symmetric and positive semidefinite matrix such that $t_{i,i} > 0$ for each i and $t_{i,j} \leqslant 0$ whenever $i \neq j$. Moreover, $\sum_{j=1}^{N_p} t_{i,j} = 0$, $i = 1, 2, \ldots, N_p$, and $\sum_{i=1}^{N_p} (T\zeta)_i = 0$ for any vector ζ. Finally, for any nonzero diagonal matrix **P**, with $\mathbf{P} \geqslant 0$, one has that $\mathbf{P}+\mathbf{T}$ is an irreducible symmetric M-matrix (see, e.g. [14], Chapter 15). Hence, $\mathbf{P}+\mathbf{T}$ is positive definite and $(\mathbf{P}+\mathbf{T})^{-1} > 0$.

Before solving system (14), one is interested in knowing if, and under which assumption, this system has a unique solution. To this purpose, note first that in each cell the volume difference corresponding to two different water levels ζ_i^α and ζ_i^β can be derived from (8) and is given by

$$V_i(\zeta_i^\beta) - V_i(\zeta_i^\alpha) = \int_{\zeta_i^\alpha}^{\zeta_i^\beta} p_i(z)\,\mathrm{d}z = \bar{p}_i(\zeta_i^\alpha, \zeta_i^\beta)(\zeta_i^\beta - \zeta_i^\alpha) \tag{15}$$

where $\bar{p}_i(\zeta_i^\alpha, \zeta_i^\beta)$, satisfying $0 \leqslant \bar{p}_i(\zeta_i^\alpha, \zeta_i^\beta) \leqslant P_i$, is the average surface area

$$\bar{p}_i(\zeta_i^\alpha, \zeta_i^\beta) = \begin{cases} p_i(\zeta_i^\alpha) & \text{if } \zeta_i^\alpha = \zeta_i^\beta \\ \dfrac{1}{\zeta_i^\beta - \zeta_i^\alpha} \displaystyle\int_{\zeta_i^\alpha}^{\zeta_i^\beta} p_i(z)\,\mathrm{d}z & \text{otherwise} \end{cases} \tag{16}$$

Moreover, the equality $\bar{p}_i(\zeta^\alpha, \zeta^\beta) = 0$ is satisfied in the only case that $V_i(\zeta_i^\alpha) = V_i(\zeta_i^\beta) = 0$.

Theorem 1
Assume that $V_i(\zeta_i) = \int_{-\infty}^{\zeta_i} p_i(z)\,\mathrm{d}z$, with $p_i(z)$ being nonnegative, nondecreasing and bounded for all i. Assume also that **T** is an irreducible, symmetric and positive semidefinite matrix such that

DOI: 10.1002/fld

$t_{i,j} \leqslant 0$ whenever $i \neq j$ and $\sum_{j=1}^{N_p} t_{i,j} = 0$ for each i. If $\sum_{i=1}^{N_p} b_i > 0$, then the solution of system (14) exists and is unique.

Proof
The existence of a solution will be established constructively by the following theorem. Regarding its uniqueness, assume that ζ^α and ζ^β are both solutions of system (14), so that $\mathbf{V}(\zeta^\alpha) + \mathbf{T}\zeta^\alpha = \mathbf{b}$ and $\mathbf{V}(\zeta^\beta) + \mathbf{T}\zeta^\beta = \mathbf{b}$. Thus,

$$[\mathbf{V}(\zeta^\beta) + \mathbf{T}\zeta^\beta] - [\mathbf{V}(\zeta^\alpha) + \mathbf{T}\zeta^\alpha] = [\bar{\mathbf{P}}(\zeta^\alpha, \zeta^\beta) + \mathbf{T}](\zeta^\beta - \zeta^\alpha) = \mathbf{0} \tag{17}$$

where $\bar{\mathbf{P}}(\zeta^\alpha, \zeta^\beta)$ is a diagonal matrix whose diagonal entries are the nonnegative averages $\bar{p}_i(\zeta_i^\alpha, \zeta_i^\beta)$. Now, since $\sum_{i=1}^{N_p} b_i > 0$, Equation (14) implies

$$\sum_{i=1}^{N_p} V_i(\zeta_i^\alpha) = \sum_{i=1}^{N_p} V_i(\zeta_i^\beta) = \sum_{i=1}^{N_p} b_i > 0$$

Consequently, some of the $V_i(\zeta_i^\alpha)$ are strictly positive, some of the $V_i(\zeta_i^\beta)$ are strictly positive and, because $p_i(z)$ are nonnegative and nondecreasing, the corresponding $\bar{p}_i(\zeta_i^\alpha, \zeta_i^\beta)$ are strictly positive. Thus $\bar{\mathbf{P}}(\zeta^\alpha, \zeta^\beta)$ is nonzero and nonnegative. Therefore, $\bar{\mathbf{P}}(\zeta^\alpha, \zeta^\beta) + \mathbf{T}$ is an M-matrix, hence nonsingular. Uniqueness ($\zeta^\alpha = \zeta^\beta$) then follows directly from (17). □

Equation (11) implies conservation of the total water volume, i.e. $\sum_{i=1}^{N_p} V_i(\eta_i^{n+1}) = \sum_{i=1}^{N_p} V_i(\eta_i^n)$. In general, however, when sources and sinks are considered and/or in presence of open boundaries where the flow is specified as a boundary condition, the new total water volume is $\sum_{i=1}^{N_p} V_i(\eta_i^{n+1}) = \sum_{i=1}^{N_p} b_i$, and includes the water volume at previous time step plus or minus the net flow in or out Ω during the time step Δt. In this case $\sum_{i=1}^{N_p} b_i > 0$ is a requirement for system (14) to be physically and mathematically compatible. Hence, existence and uniqueness of a solution is certainly guaranteed when the problem is correctly posed.

If the water surface elevation is specified as a boundary conditions at some boundary polygons, then the corresponding Equations (12) are removed from the system and the resulting matrix $\mathbf{T}$ becomes positive definite. Consequently, the inequality $\sum_{i=1}^{N_p} b_i > 0$ is not required to show existence and uniqueness of the solution of system (14).

4.2. A Newton-type method

From Equation (8) one has that the derivative of $V_i(\zeta_i)$ is the possibly discontinuous surface wet area $p_i(\zeta_i)$. Nevertheless, an efficient Newton-type algorithm for solving system (14) is given by

$$\zeta^{m+1} = \zeta^m - [\mathbf{P}(\zeta^m) + \mathbf{T}]^{-1}[\mathbf{V}(\zeta^m) + \mathbf{T}\zeta^m - \mathbf{b}], \quad m = 0, 1, 2, \ldots \tag{18}$$

where m now denotes the iteration index (not to be confused with the time step) and $\mathbf{P}(\zeta^m)$ is a diagonal matrix whose diagonal entries are the surface wet areas $p_i(\zeta_i^m)$.

Theorem 2
Assume that $V_i(\zeta_i) = \int_{-\infty}^{\zeta_i} p_i(z)\,\mathrm{d}z$, with $p_i(z)$ being nonnegative, nondecreasing and bounded for all i. Assume also that $\mathbf{T}$ is an irreducible, symmetric and positive semidefinite matrix such that

DOI: 10.1002/fld

$t_{i,j} \leqslant 0$ whenever $i \neq j$ and $\sum_{j=1}^{N_p} t_{i,j} = 0$ for each i. If $\sum_{i=1}^{N_p} b_i > 0$ and $\mathbf{P}(\zeta^0) \neq 0$, then the iterative scheme (18) converges to the exact solution of system (14).

Proof

With the specified assumptions it will be shown, by induction, that $\mathbf{P}(\zeta^m) + \mathbf{T}$ is an M-matrix, thus nonsingular for all $m \geqslant 0$.

In fact, since $\mathbf{P}(\zeta^0) \neq 0$ and $\mathbf{P}(\zeta^0) \geqslant 0$, and because $\mathbf{T}$ is irreducible, one has that $\mathbf{P}(\zeta^0) + \mathbf{T}$ is an M-matrix, hence nonsingular and ζ^1 is uniquely obtained from (18).

Next, for any $m \geqslant 1$ one assumes that $\mathbf{P}(\zeta^{m-1}) + \mathbf{T}$ is nonsingular. Hence ζ^m is the unique solution of

$$[\mathbf{P}(\zeta^{m-1}) + \mathbf{T}](\zeta^m - \zeta^{m-1}) + \mathbf{V}(\zeta^{m-1}) + \mathbf{T}\zeta^{m-1} = \mathbf{b} \tag{19}$$

Similarly, the iterative scheme (18) yields

$$[\mathbf{P}(\zeta^m) + \mathbf{T}](\zeta^{m+1} - \zeta^m) + \mathbf{V}(\zeta^m) + \mathbf{T}\zeta^m = \mathbf{b} \tag{20}$$

By equating the left-hand sides of Equations (19) and (20), after simplifications, one gets

$$[\mathbf{P}(\zeta^m) + \mathbf{T}](\zeta^{m+1} - \zeta^m) + \boldsymbol{\xi}^m = 0 \tag{21}$$

where the vector ξ^m can be written as

$$\begin{aligned} \xi^m &= \mathbf{V}(\zeta^m) - \mathbf{V}(\zeta^{m-1}) - \mathbf{P}(\zeta^{m-1})(\zeta^m - \zeta^{m-1}) \\ &= [\bar{\mathbf{P}}(\zeta^{m-1}, \zeta^m) - \mathbf{P}(\zeta^{m-1})](\zeta^m - \zeta^{m-1}) \end{aligned} \tag{22}$$

Since $p_i(z)$ are nondecreasing functions of z, Equation (16) implies that where $\zeta^m \geqslant \zeta^{m-1}$ one has $\bar{\mathbf{P}}(\zeta^{m-1}, \zeta^m) \geqslant \mathbf{P}(\zeta^{m-1})$ and where $\zeta^m < \zeta^{m-1}$ one has $\bar{\mathbf{P}}(\zeta^{m-1}, \zeta^m) \leqslant \mathbf{P}(\zeta^{m-1})$. Thus $\xi^m \geqslant 0$, $m = 1, 2, \ldots$.

Moreover, an alternative expression for ξ^m can be derived from Equations (20) and (21) and is given by

$$\xi^m = \mathbf{V}(\zeta^m) + \mathbf{T}\zeta^m - \mathbf{b} \tag{23}$$

Next, by summing up all terms on both sides of Equation (23), one obtains

$$\sum_{i=1}^{N_p} V_i(\zeta_i^m) = \sum_{i=1}^{N_p} (b_i + \xi_i^m) \geqslant \sum_{i=1}^{N_p} b_i > 0$$

thus, some of the $V_i(\zeta_i^m)$ are strictly positive and, consequently, the corresponding $p_i(\zeta_i^m)$ must be positive. Therefore, $\mathbf{P}(\zeta^m) + \mathbf{T}$ is an M-matrix and ζ^{m+1} is uniquely obtained from (18).

Finally, since $\mathbf{P}(\zeta^m) + \mathbf{T}$ is an irreducible M-matrix one has $[\mathbf{P}(\zeta^m) + \mathbf{T}]^{-1} > 0$. Moreover, because $\xi^m \geqslant 0$, Equation (21) implies $\zeta^{m+1} \leqslant \zeta^m$ and, therefore, $\mathbf{P}(\zeta^{m+1}) \leqslant \mathbf{P}(\zeta^m)$. Thus, the iterative scheme (18) generates a nonnegative and monotonically decreasing, hence converging, sequence $\mathbf{P}(\zeta^m)$. Consequently, $\bar{\mathbf{P}}(\zeta^{m-1}, \zeta^m) \to \mathbf{P}(\zeta^{m-1})$ and Equation (22) implies $\xi^m \to 0$. Convergence of ζ^m to the exact solution of system (14) then results from Equation (23). □

If $\mathbf{P}(\eta^n) \neq \mathbf{0}$, the assumption $\mathbf{P}(\zeta^0) \neq 0$ can be easily satisfied by choosing $\zeta^0 = \eta^n$ as an initial guess. In this way one, or just a few iterations, will be sufficient to solve system (14). In the

DOI: 10.1002/fld

particular case that no wetting or drying takes place in Ω between time steps n and $n+1$, by using $\zeta^0=\eta^n$ as an initial guess, one has $\mathbf{P}(\zeta)=\mathbf{P}(\zeta^0)$, and the exact solution of (14) is obtained in only one iteration. In this case, in fact, Equations (14) and (15) yield $\mathbf{V}(\zeta^0)=\mathbf{b}-\mathbf{T}\zeta-\mathbf{P}(\zeta^0)(\zeta-\zeta^0)$. Hence, for $m=0$, the iterative scheme (18) simplifies to $\zeta^1=\zeta$.

Note that if the water surface elevation is specified as a boundary condition at some boundary polygon, the resulting matrix $\mathbf{T}$ becomes positive definite. In this case the assumption $\sum_{i=1}^{N_p} b_i>0$ can be removed and convergence of the iterative scheme (18) is guaranteed with any initial guess.

From a practical point of view, since $\mathbf{P}(\zeta^m)+\mathbf{T}$ is a symmetric M-matrix, it is positive definite. Thus, each iteration (18) can be efficiently performed by using a preconditioned conjugate gradient method (see, e.g. [15]). Consequently, a properly coded numerical model that includes the proposed wetting and drying algorithm can be robust and very efficient.

With the specified assumptions if, in addition, the bathymetry is given as a piecewise constant function $h(x,y)=h_i, (x,y)\in\Omega_i,\ \ i=1,2,\ldots,N_p$ (without any subgrid detail), then the water volumes are $V_i(\zeta_i)=P_i\max(0,h_i+\zeta_i)$ and system (14) becomes piecewise linear. In such a case the Newton-type algorithm (18) can be shown to converge to the exact solution in a finite number of iterations (see [16] for details).

4.3. Linear vs nonlinear formulation

When the free-surface does not intersect the bathymetry, the proposed algorithm reduces to the one traditionally used in semi-implicit methods [9]. In fact, if $h(x,y)+\eta_j^n\geqslant 0$ along the jth edge then, by denoting with h_j the edge-averaged bathymetric value, and by setting $\bar{H}_j^n=h_j+\eta_j^n$, one has $H_j^n=\bar{H}_j^n$. Consequently, Equation (10) can be written as

$$\bar{H}_j^n u_j^{n+1}=\bar{H}_j^n G_j^n-\theta g\bar{H}_j^n\frac{\Delta t}{\delta_j}[\eta_{i(j,2)}^{n+1}-\eta_{i(j,1)}^{n+1}]-\Delta t\gamma_j^n u_j^{n+1} \tag{24}$$

Similarly, by denoting with h_i the cell-averaged bathymetric value, if $h(x,y)+\eta_i^n\geqslant 0$ and $h(x,y)+\eta_i^{n+1}\geqslant 0$ for all $(x,y)\in\Omega_i$, then $V_i(\eta_i^n)=P_i(h_i+\eta_i^n)$, $V_i(\eta_i^{n+1})=P_i(h_i+\eta_i^{n+1})$ and Equation (11) simplifies to

$$P_i\eta_i^{n+1}=P_i\eta_i^n-\Delta t\sum_{\ell=1}^{S_i}s_{i,\ell}\lambda_{j(i,\ell)}\bar{H}_{j(i,\ell)}^n[\theta u_{j(i,\ell)}^{n+1}+(1-\theta)u_{j(i,\ell)}^n] \tag{25}$$

Then, formal substitution of the expressions for u_j^{n+1} from Equation (24) into (25) yields a discrete *linear* wave equation for η_i^{n+1} that is given by

$$\begin{aligned}P_i\eta_i^{n+1}-g\Delta t^2\theta^2\sum_{\ell=1}^{S_i}\frac{\lambda_{j(i,\ell)}}{\delta_{j(i,\ell)}}\left(\frac{\bar{H}^2}{\bar{H}+\Delta t\gamma}\right)_{j(i,\ell)}^n(\eta_{n(i,\ell)}^{n+1}-\eta_i^{n+1})\\ =P_i\eta_i^n-\Delta t\sum_{\ell=1}^{S_i}s_{i,\ell}\lambda_{j(i,\ell)}\bar{H}_{j(i,\ell)}^n\left[\theta\frac{\bar{H}G}{\bar{H}+\Delta t\gamma}+(1-\theta)u\right]_{j(i,\ell)}^n,\quad i=1,2,\ldots,N_p\end{aligned} \tag{26}$$

Hence, if Ω is fully wet at both time levels n and $n+1$, then Equations (12) and (26) are equivalent. In this case, the subgrid specification has no influence on the resulting flow which is determined only by the edge-averaged bathymetry h_j.

DOI: 10.1002/fld

A substantial difference between the present algorithm and the one traditionally used in linear semi-implicit methods arises in the presence of wetting and/or drying. Note, in fact, that Equations (6) and (8) give

$$V_i(\eta_i^n)=\int_{\Omega_i}\max[0,h(x,y)+\eta_i^n]\,\mathrm{d}x\,\mathrm{d}y\geqslant\int_{\Omega_i}[h(x,y)+\eta_i^n]\,\mathrm{d}x\,\mathrm{d}y=P_i(h_i+\eta_i^n)$$

Thus, because $V_i(\eta_i^n)\geqslant P_i(h_i+\eta_i^n)$ with strict inequality when the free-surface level η_i^n intersects the bathymetry within the ith polygon, the equivalence between Equations (11) and (25) is no longer valid in those polygons where wetting or drying is in progress during the transition from time level n to $n+1$.

Since the linear formulation (26) uses bathymetric information only at polygon edges, each water column behaves as bottomless. The linear formulation, in fact, allows the development of un-physical negative water depths. The resulting volume over-drainage in the dry region is compensated by an artificial increase of water volume in the wet region. This discrepancy may also cause undesired errors in mass balance of transported scalars when a mass transport scheme that requires consistency with continuity is coupled with a linear hydrodynamic model (see, e.g. [17]).

With the proposed mildly nonlinear formulation (12) a correct mass balance is always achieved in wet cells, as well as in cells of transition from wet to dry and from dry to wet, regardless of the specified bathymetric details. Nonnegative water volumes and nonnegative water depths are always assured everywhere. Additionally, the specification of bathymetric details at subgrid level plays an important role to obtain an accurate mass balance in the wetting and drying region where any polygon is allowed to be wet, partially wet or dry.

Moreover, Equations (6) and (9) give

$$H_j(\eta_j^n)=\frac{1}{\lambda_j}\int_{s_j^1}^{s_j^2}\max[0,h(x(s),y(s))+\eta_j^n]\,\mathrm{d}s\geqslant\frac{1}{\lambda_j}\int_{s_j^1}^{s_j^2}[h(x(s),y(s))+\eta_j^n]\,\mathrm{d}s=\bar{H}_j^n$$

Thus, since $H_j^n\geqslant\bar{H}_j^n$ with strict inequality when the free-surface level η_j^n intersects the bathymetry along the jth edge, $\bar{H}_j^n$ underestimates the correct edge-averaged water depth in the wetting and drying region. Consequently, a reduced celerity will result in linear semi-implicit models, producing, e.g. oscillations known as *artificial bores*. The specification of the bathymetric function $h(x,y)$ at subgrid level permits a more accurate determination of the edge-averaged water depth H_j^n, which allows a more gradual transition from wet to dry grid points. This is particularly the case in flows over complex geometries.

The enhanced ability of the present formulation to account for bathymetric details with an arbitrarily fine subgrid resolution, makes the present algorithm applicable to one-dimensional flows in open channels with arbitrary cross-section [18]. Additionally, the proposed formulation extends quite naturally to hydrostatic, three-dimensional flows (see, e.g. [9]). In this latter case, the resulting mildly nonlinear system for the water surface elevation has essentially the same structure and size as (12). Hence, three-dimensional flows subject to wetting and drying can be obtained by the present algorithm with a reasonable increase of the corresponding computational effort.

DOI: 10.1002/fld

5. NUMERICAL TEST

The present algorithm has been successfully tested on several two- and three-dimensional realistic field scale problems with different flow regimes and complexity. To be quantitatively precise, a simple and yet severe test-case with known analytical solution is considered next. The flow is *frictionless* and is determined by the initial conditions, by the nonlinear advective terms, by the Coriolis acceleration and by the hydrostatic pressure. Wetting and drying is also included.

The flow takes place in a basin described by a paraboloid of revolution given by

$$h(x, y) = h_0 \left(1 - \frac{r}{L^2}\right) \tag{27}$$

where h_0 and L are positive constants and $r = \sqrt{x^2 + y^2}$ is the distance from the origin (see Figure 2).

A nontrivial analytical solution, whose free-surface is a paraboloid of revolution, is that for a long resonating wave. This solution was given in [19] for the two-dimensional shallow water equations and recently extended to three-dimensional problems in [20]. In polar coordinates (r, ϑ) the exact two-dimensional solution is given by

$$u_r = \frac{\omega r A \sin \omega t}{2(1 - A \cos \omega t)} \tag{28}$$

$$u_\vartheta = \frac{fr}{2(1 - A \cos \omega t)} (\sqrt{1 - A^2} + A \cos \omega t - 1) \tag{29}$$

$$\eta = h_0 \left\{ \frac{\sqrt{1 - A^2}}{1 - A \cos \omega t} - 1 - \frac{r^2}{L^2} \left[\frac{1 - A^2}{(1 - A \cos \omega t)^2} - 1 \right] \right\} \tag{30}$$

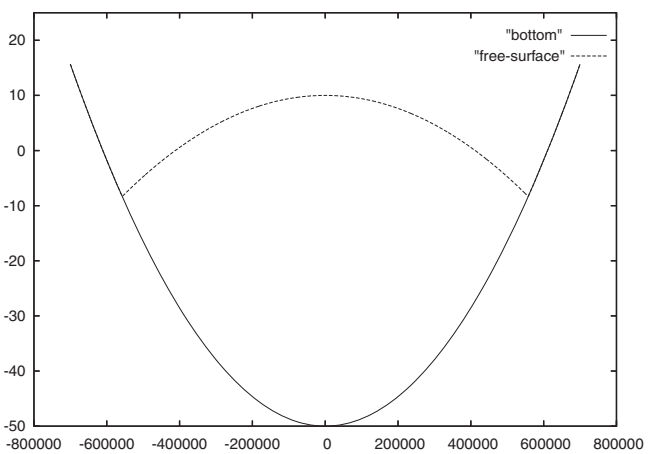

Figure 2. Cross-sectional view of the parabolic basin test.

DOI: 10.1002/fld

where, by setting $\eta_0=\eta(0,0,0)$, the constant A is given by

$$A=\frac{(h_0+\eta_0)^2-h_0^2}{(h_0+\eta_0)^2+h_0^2}$$

and, for a specified frequency $\omega>f$, L is given by

$$L=\sqrt{\frac{8gh_0}{\omega^2-f^2}}$$

Equations (28)–(29) show that the radial component of the velocity u_r is independent of the Coriolis acceleration, while the tangential component u_ϑ is proportional to f. Moreover, the total water depth is given by

$$H=h_0\left[\frac{\sqrt{1-A^2}}{1-A\cos\omega t}-\frac{r^2(1-A^2)}{L^2(1-A\cos\omega t)^2}\right]$$

so that the shoreline is a circle whose center coincides with the center of the basin and the time-dependent radius $R(t)$ given by

$$R(t)=L\sqrt{\frac{1-A\cos\omega t}{\sqrt{1-A^2}}} \tag{31}$$

Hence, the permanently wet region is confined within the disk where $r<R_{\min}$ and the wetting and drying takes place within the region $R_{\min}\leqslant r<R_{\max}$, with $R_{\max,\min}=L\sqrt{(1\pm A)/\sqrt{(1-A^2)}}$.

The chosen parameters h_0, f, ω and η_0 have been taken from Reference [20] where a realistic environmental flow was simulated. Specifically, by setting $h_0=50\,\mathrm{m}$, $\eta_0=2\,\mathrm{m}$, a latitude of 45° North and $\omega=2\pi/(12\times3600)$, the resulting wave period is $T=12\,\mathrm{h}$, $L=610\,\mathrm{km}$, $R_{\min}=598\,\mathrm{km}$ and $R_{\max}=623\,\mathrm{km}$.

In Reference [20] a good agreement between the numerical and the exact solution was reported after simulating two time periods with a time step size $\Delta t=100\,\mathrm{s}$ and a refined grid with $\lambda_j\leqslant800\,\mathrm{m}$ to cover the wetting and drying region. Here a much coarser grid is constructed by taking mixed, triangular and quadrilateral polygons in such a fashion that their vertices all lie on concentric circles equally spaced at a distance $\Delta r=10\,\mathrm{km}$ and such that their sides never exceed Δr (see Figure 3). No grid refinement is used to cover the wetting and drying region, except that each polygon is further partitioned in 10 subpolygons, where the bathymetric data are specified with higher resolution. The wetting and drying region is located within four rings of trapezoidal polygons whose oblique sides are $\Delta r=10\,\mathrm{km}$. The innermost ring never gets completely dry and the outermost ring never gets completely wet. The overall grid contains $N_{\mathrm{p}}=19\,349$ polygons and $N_{\mathrm{s}}=38\,192$ sides.

It is worth noting that the total water volume is conserved. In fact, $\sum_{i=1}^{N_{\mathrm{p}}}V_i(\eta_i^n)=\sum_{i=1}^{N_{\mathrm{p}}}V_i(\eta_i^0)>0$ for all n. Hence, when η^n is used as initial guess for the iterative scheme (18), the conditions required by Theorem 2 are fulfilled and convergence is always guaranteed. As a matter of fact, solving system (14) with an accuracy of $10^{-14}\,\mathrm{m}$ requires an average of two iterations per time step. In this problem matrix $\mathbf{T}$ is always positive semidefinite, hence singular.

The present simulation is started with the initial conditions taken from (28)–(30) with $t=0$. The numerical solution is then computed for 10 time periods with a large time step $\Delta t=900\,\mathrm{s}$. Figures 4

DOI: 10.1002/fld

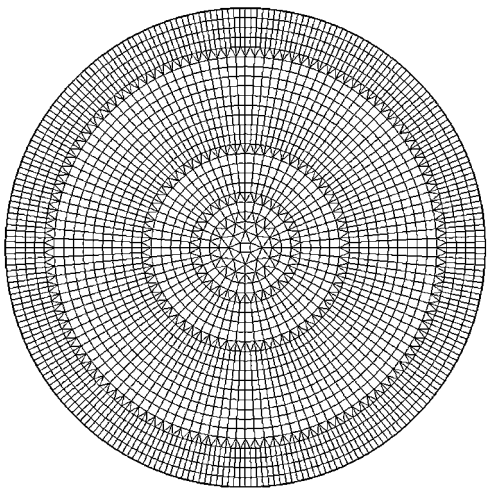

Figure 3. Unstructured grid arrangement for a paraboloid of revolution.

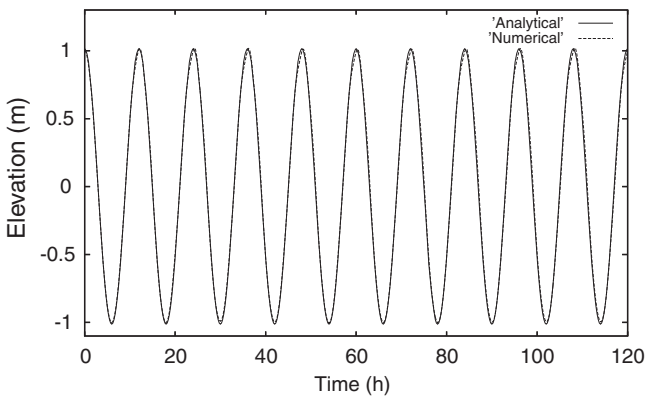

Figure 4. Free-surface elevation time series at $r = 300\,\text{km}$.

and 5 show the time series of the computed and the exact values of the free-surface elevation at $r = 300\,\text{km}$ and $r = L$, respectively. It is to be noted that the location $r = L$ becomes dry during about half period. Accordingly, during the dry phase the computed water depth at this station is zero. The numerical and the analytical solution almost overlaps everywhere at $r = 300\,\text{km}$, whereas a slight phase shift and some small differences in the peaks can be observed at $r = L$.

The accurate simulation of the wetting and drying dynamic is rather crucial in this problem because, in absence of friction, incorrect wave reflection from the shoreline unavoidably propagates everywhere without damping. For comparison, Figure 6 shows the free-surface profile along the basin diameter computed after 10 time periods with and without subgrid refinements. The development of higher harmonics obtained without subgrid refinements is clearly shown.

DOI: 10.1002/fld

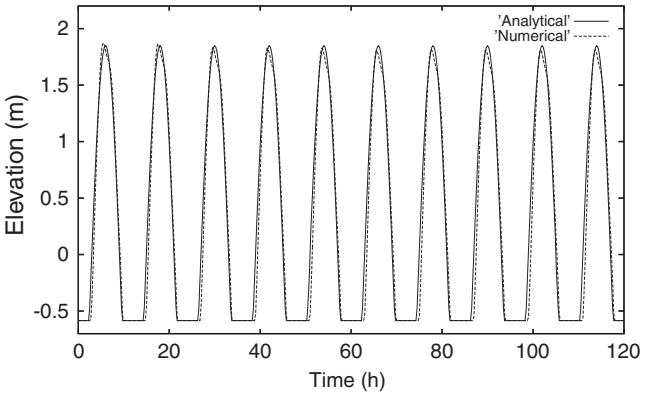

Figure 5. Free-surface elevation time series at $r = L$.

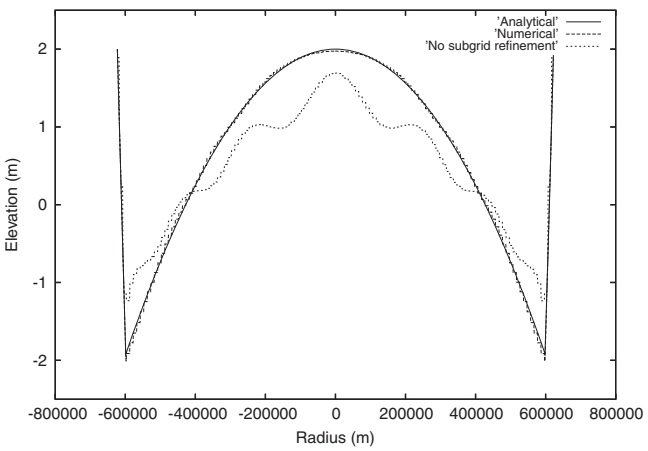

Figure 6. Free-surface profile after 10 time periods.

Figure 7 shows the computed fraction of the wet area. Again, a slight phase shift and a small discrepancy near the peaks are shown by the computed results. However, given that the wetting and drying region has been covered by an extremely coarse mesh, the above results can be considered as remarkably accurate.

Finally, Figures 8 and 9 show the time series of the computed and the exact values of the velocity u_r and u_ϑ, respectively, at $r = 300\,\text{km}$. As shown in these figures, an exceptionally good agreement between the analytical and the numerical solutions is achieved.

This calculation was performed on a PC with a 2.16 GHz Core 2 Duo processor using an OpenMP parallel implementation. The required CPU time for 10 tidal cycles was 84 s and the corresponding wall clock time was only 42 s.

Overall, these results confirm that, with the proposed nonlinear formulation for the numerical simulation of wetting and drying, an acceptable accuracy and a precise volume balance at the subgrid level can be obtained without resorting to costly and unnecessary grid refinements.

DOI: 10.1002/fld

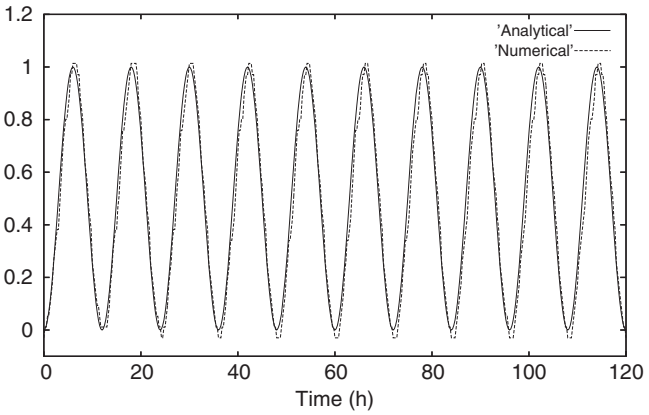

Figure 7. Wet area time series.

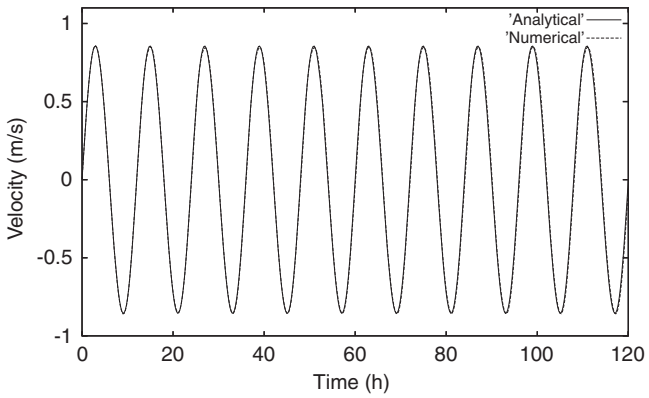

Figure 8. Time series of u_r at $r = 300\,\text{km}$.

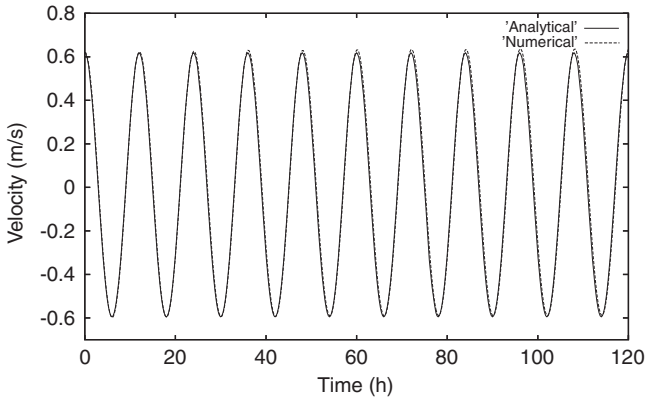

Figure 9. Time series of u_ϑ at $r = 300\,\text{km}$.

DOI: 10.1002/fld

6. CONCLUSIONS

An efficient semi-implicit algorithm for simulating wetting and drying in two-dimensional shallow water flows has been derived from the governing differential equations.

The spatial discretization consists of an unstructured grid that provides a great flexibility for fitting boundaries and for local mesh refinements. Additionally, an arbitrarily fine spatial resolution at subgrid level is permitted and recommended to obtain an accurate mass balance in shallow flows over complex geometries.

The dry region is recognized by having exactly zero water depth and the transition from wet to dry and from dry to wet can involve several cells without time step limitations.

A detailed analysis has been developed assuring robustness to a properly coded numerical model. The resulting algorithm is numerically stable, relatively simple and very efficient.

REFERENCES

1. Balzano A. Evaluation of methods for numerical simulation of wetting and drying in shallow water flow models. *Coastal Engineering* 1998; **34**:83–107.
2. Cea L, Puertas J, Vázquez-Cendón ME. Depth averaged modelling of turbulent shallow water flow with wet–dry fronts. *Archives of Computational Methods in Engineering* 2006; **11**:1–50.
3. Leendertse JJ. A water-quality simulation model for well-mixed estuaries and coastal seas. Principles of computation. *Rand*, *Santa Monica* 1970; **1**:RM-6230-RC.
4. Stelling GS. On the construction of computational methods for shallow water equations. *Rijkswaterstaat Communications* 1984; **35r1984**:226.
5. Lesser GR, Roelvink JA, van Kester JATM, Stelling GS. Development and validation of a three-dimensional morphological model. *Coastal Engineering* 2004; **51**:883–915.
6. van't Hof B, Vollebregt EAH. Modelling of wetting and drying of shallow water using artificial porosity. *International Journal for Numerical Methods in Fluids* 2005; **48**:1199–1217.
7. Casulli V. Semi-implicit finite difference methods for the two-dimensional shallow water equations. *Journal of Computational Physics* 1990; **86**:56–74.
8. Casulli V, Cheng RT. Semi-implicit finite difference methods for three-dimensional shallow water flow. *International Journal for Numerical Methods in Fluids* 1992; **15**:629–648.
9. Casulli V, Walters RA. An unstructured grid, three-dimensional model based on the shallow water equations. *International Journal for Numerical Methods in Fluids* 2000; **32**:331–348.
10. Stelling GS, Duynmeyer SPA. A staggered conservative scheme for every Froude number in rapidly varied shallow water flows. *International Journal for Numerical Methods in Fluids* 2003; **43**:1329–1354.
11. Walters RA. Coastal ocean models: two useful finite element methods. *Continental Shelf Research* 2005; **25**: 775–793.
12. Casulli V, Zanolli P. Semi-implicit numerical modeling of non-hydrostatic free-surface flows for environmental problems. *Mathematical and Computer Modelling* 2002; **36**:1131–1149.
13. Casulli V, Cattani E. Stability, accuracy and efficiency of a semi-implicit method for three-dimensional shallow water flow. *Computers and Mathematics with Applications* 1994; **27**:99–112.
14. Lancaster P, Tismenetsky M. *The Theory of Matrices* (2nd edn). Academic Press: London, 1985.
15. Golub GH, van Loan CF. *Matrix Computations* (3rd edn). J. Hopkins: London, 1996.
16. Brugnano L, Casulli V. Iterative solution of piecewise linear systems. *SIAM Journal on Scientific Computing* 2008; **30**:463–472.
17. Casulli V, Zanolli P. High resolution methods for multidimensional advection–diffusion problems in free-surface hydrodynamics. *Ocean Modelling* 2005; **10**:137–151.
18. Aldrighetti E, Zanolli P. A high resolution scheme for fows in open channels with arbitrary cross-sections. *International Journal for Numerical Methods in Fluids* 2005; **47**:817–824.
19. Thacker WC. Some exact solutions to the nonlinear shallow water equations. *Journal of Fluid Mechanics* 1981; **107**:499–508.
20. Casulli V, Zanolli P. Comparing analytical and numerical solution of nonlinear two and three dimensional hydrostatic flows. *International Journal for Numerical Methods in Fluids* 2007; **53**:1049–1062.

DOI: 10.1002/fld